Astron. Nachr. / AN **330**, No. 00, 960 – 965 (2009) / **DOI** 10.1002/asna.200911272

arXiv:0910.2643v1 [astro-ph.CO] 14 Oct 2009

Metallicity Gradients - Mass Dependency in Dwarf Elliptical Galaxies

M. Koleva[1,2,3,⋆], **Ph. Prugniel**[3], **S. De Rijcke**[4], **W. W. Zeilinger**[5], and **D. Michielsen**[4]

[1] Instituto de Astrofísica de Canarias, La Laguna, E-38200 Tenerife, Spain
[2] Departamento de Astrofísica, Universidad de La Laguna, E-38205 La Laguna, Tenerife, Spain
[3] Université Lyon 1, Villeurbanne, F-69622, France; CRAL, Observatoire de Lyon, St. Genis Laval, F-69561, France; CNRS, UMR 5574
[4] Sterrenkundig Observatorium, Ghent University, Krijgslaan 281, S9, B-9000 Ghent, Belgium
[5] Institut für Astronomie, Universität Wien, Türkenschanzstraße 17, A-1180 Wien, Austria

Received 2009 Jul 14, accepted 2009 Sep 14
Published online 2009 Oct 20

Key words galaxies: dwarf – galaxies: structure – galaxies: evolution

The formation and evolution of galaxies is imprinted on their stellar population radial gradients. Two recent articles present conflicting results concerning the mass dependence of the metallicity gradients for early-type dwarf galaxies. On one side, Spolaor et al. show a tight positive correlation between the total metallicity $[Z/H]$ and the mass. On the other side, in a distinct sample⋆⋆, we do not find any trend involving $[Fe/H]$ (Koleva et al.). In order to investigate the origin of the discrepancy, we examine various factors that may affect the determination of the gradients: namely the sky subtraction and the signal-to-noise ratio. We conclude that our detection of gradients are well above the possible analysis biases. Then, we measured the $[Mg/Fe]$ relative abundance profile and found moderate gradients. The derived $[Z/H]$ gradients scatter around -0.4 dex/r_e. The two samples contain the same types of objects and the reason of the disagreement is still not understood.

© 2009 WILEY-VCH Verlag GmbH & Co. KGaA, Weinheim

1 Introduction

The stellar populations of galaxies hold a fossil record of their formation and evolution. Their study may allow to discriminate between the various formation scenarios predicting different spatial gradients and different relations between the gradients and the mass of the galaxy.

In the classical monolithic scenario, galaxies formed in a dissipative collapse (Larson, 1974; Arimoto & Yoshii, 1987), where stars remain on their orbits and do not mix. The gas, enriched in metals from the evolved stars, flows into the centre, generating negative metallicity gradients (*i.e.* higher metal content in the centre than in the outskirts). The chemo-dynamical simulations Matteucci & Tornambe (1987, see also Kawata & Gibson, 2003) predict, that due to their small potential, dwarf galaxies, are unable to retain metals and thus their gradients are shallower or almost inexistent. Therefore relations between the mass and the metallicity or the metallicity gradient are expected.

A competing (or complementary) formation scenario is the hierarchical clustering (e.g. Cole et al., 1994), where small dark matter halos merge to produce bigger galaxies. It may be thought that these violent events mix the stellar population and erase the gradients (e.g. White, 1980), but some simulations (e.g. di Matteo et al., 2009), at variance, show a gradient preservation, due to the violent relaxation which does not mix the orbits.

The interpretation of the metallicity gradients is not straightforward. Nevertheless, gradients observation could constrain model's predictions. Several studies on big samples of giant elliptical galaxies have been already performed (e.g. Sánchez-Blázquez et al., 2006). However, due to their low-surface brightness, the dwarf galaxies, are still very much 'terra incognita'.

Recently we published a paper on the stellar content of 16 dwarf galaxies in the Fornax cluster and in groups (Koleva et al., 2009a). One of our main conclusions was that most of our galaxies hold a strong negative metallicity gradient. The star formation history analyses revealed that these gradients are built at early epochs. We did not find any correlation between our gradients and the velocity dispersion (proxy of the mass) in our sample (Fig.1). However, this result is challenged by a recent letter from Spolaor et al. (2009), using a sample of 14 dwarfs in the Virgo and Fornax clusters observed with GMOS at the Gemini South telescope in medium resolution, long-slit, optical spectroscopy.

To analyse their data, Spolaor et al. (2009) binned them along the slit direction to achieve a minimum signal-to-noise of 30 @ 5200 Å. They measured Lick indices (Worthey et al., 1994; Worthey & Ottaviani, 1997) and derived ages and chemical compositions by comparing to the Thomas et al. (2004) single stellar population (SSP) models,

⋆ Corresponding author: e-mail: koleva@iac.es

⋆⋆ Based on observations made with ESO telescopes at La Silla Paranal observatory under program ID076.B-0196

WILEY InterScience DISCOVER SOMETHING GREAT

© 2009 WILEY-VCH Verlag GmbH & Co. KGaA, Weinheim

using their own method (Proctor & Sansom, 2002). They estimated the gradients performing a linear least-squares fit to the radial metallicity profile weighted by their errors. The fit was done in logarithmic space of the radius, $\Delta[Z/H]/\Delta\log(r/r_e)$, where r varies from 1 arcsec to one effective radius (r_e).

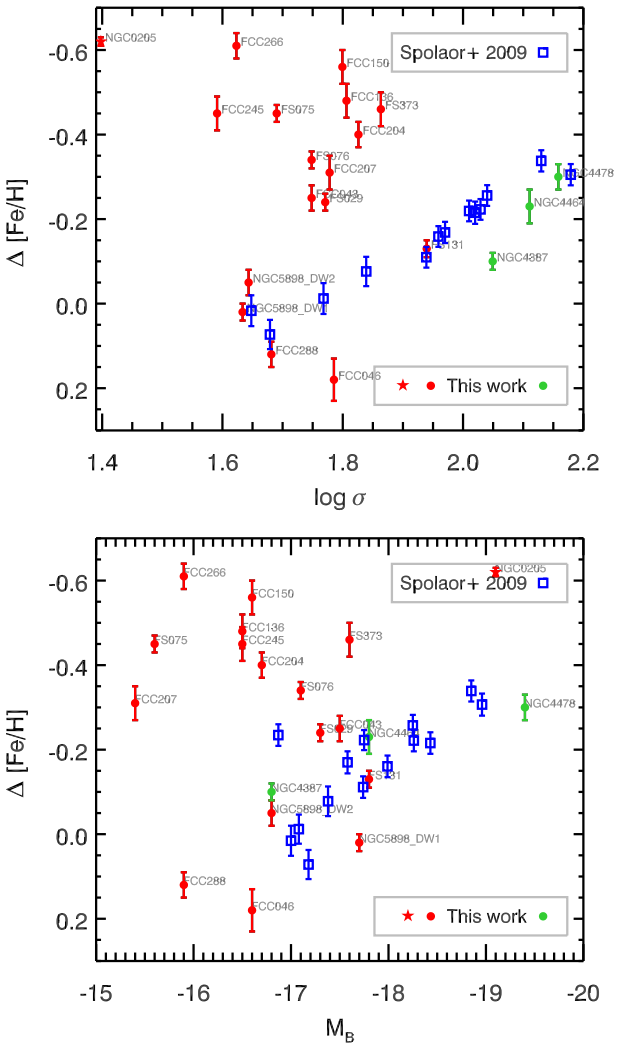

Fig. 1 Metallicity gradients *vs.* σ and M_B (top and bottom respectively) of the 2 samples of dwarf elliptical galaxies, one from Spolaor et al. (2009, blue, open squares) and other is this work (filled symbols). Green circles are galaxies from Vazdekis et al. (2001), red circles from Koleva et al. (2009a) and a red star for NGC 205(Simien & Prugniel, 2002). The names of our galaxies are also plotted.

There is no galaxy in common between the two samples and the causes of the disagreement may be multiple: choice of the sample, data reduction or analysis issue. The primary purpose of the present paper is to explore these possibilities. In order to directly compare our results with Spolaor et al. (2009) we will determine our metallicity gradients in an identical way.

In Sect.2 we present the sample, observations and analysis. In Sect.3.1 we investigate the systematics (signal-to-noise ratio, bad sky-subtraction) which may affect the derived metallicity gradients. As Spolaor et al. used the total metallicity $[Z/H]$we also measured $[Mg/Fe]$ and discuss the differences between $\Delta[Fe/H]$ and $\Delta[Z/H]$ in Sect.3.2.

2 Data and analysis

For the purpose of the present paper we collected 20 early-type galaxies (Table 1) with velocity dispersions less than 150 km s^{-1} from three different data sets (VLT, OHP and WHT). We analysed them with the same method.

2.1 OHP data

We used long slit data of NGC 205 (Simien & Prugniel, 2002), which were taken with CARELEC spectrograph on 1.93 m telescope in Observatoire de Haute-Provence (OHP). The observations were carried from January 2001 to January 2003 and are partly used in Simien & Prugniel (2002) to derive the internal kinematics. The slit width was set to 1.5″, which results in an instrumental broadening of R = 5050 (FWHM, or $\sigma_{ins} \approx 25$ km s^{-1}). The wavelength range covers $\lambda\lambda$ 4700 – 5600 Å. NGC 205 is an emblematic galaxy for the dwarf elliptical class.

2.2 VLT data

We obtained long slit spectra of 16 dwarfs elliptical galaxies (dE) with FORS1,2 mounted on the VLT. These galaxies are situated in the Fornax cluster and the NGC 5044, NGC 5898 and NGC 3258 groups, *i.e.* in different environments. This sample covers a diversity of dwarfs: nucleated, non-nucleated, with or without spiral substructures, with or without gas (Koleva et al., 2009a, table1). These dwarfs have M_B between -17.8 and -15.4, while their velocity dispersion[1] ranges from 39.5 to 87.0 km s^{-1}. In other words they are similar to the dEs prototype - NGC 205.

The group galaxies were observed with FORS2 with the GRIS1200g+96 grism, resulting in $\lambda\lambda$ 3300-6200 Å and σ_{ins} = 74 km s^{-1}. The Fornax data were observed with the GRIS 600B+22 grism on FORS1, which results in $\lambda\lambda$ 4335-5640 Å and σ_{ins} = 64 km s^{-1}at 5200 Å.

2.3 VAKU sample

We also used three of the 6 Virgo cluster galaxies analysed in Vazdekis et al. (2001). These three objects are situated in the transition region between normal and dwarf elliptical galaxies ($\sigma \approx 120$ km s^{-1}and $M_B \sim$-18). The long slit observations were made with the William Herschel Telescope (WHT) in La Palma. The wavelength coverage is $\lambda\lambda \approx 4000 - 5000$ Å, and the instrumental resolution is 2.4 Å, or R ≈ 2000.

[1] luminosity weighted mean velocity dispersion from De Rijcke et al. 2005

© 2009 WILEY-VCH Verlag GmbH & Co. KGaA, Weinheim

Table 1 Properties of our galaxies sample. In column 1 we list the galaxies' names, in columns 2 and 3 the equatorial coordinates, in column 4 the *B*-band apparent magnitude m_B, in column 5 the Schlegel galactic extinction (Schlegel et al., 1998, ABG,PLEINPOT), in column 6 the radial velocities (measured with ULySS), in column 7 the k-correction (from COCOR, PLEINPOT, using the listed cz values), in column 8 the absolute magnitudes M_B in *B*-band (computed as described in the text), in column 9 the effective radius derived from the *R*-band images (De Rijcke et al., 2005), in column 10 the luminosity-weighted velocity dispersion (De Rijcke et al., 2005), in column 11 the metallicity gradients (derived as described in the text).

Object	α_{J2000}	δ_{J2000}	m_B	A_B	cz [km s^{-1}]	K	M_B	r_e [$''$]	σ [km s^{-1}]	Δ[Fe/H] [dex]
NGC 205	00 40 22.1	+41 41 07	8.89[a]	0.37	-234	+0.00	-19.1	150.0[b]	25[c]	-0.62 $\pm$ 0.01
NGC 4387	12 25 41.7	+12 48 38	12.97[a]	0.14	+586	-0.01	-16.8	26.0[d]	112[d]	-0.10 $\pm$ 0.02
NGC 4464	12 29 21.3	+08 09 24	13.56[a]	0.09	+1266	-0.02	-17.8	6.0[d]	129[d]	-0.23 $\pm$ 0.04
NGC 4478	12 30 17.8	+12 19 37	12.16[a]	0.10	+1390	-0.02	-19.4	17.0[d]	144[d]	-0.30 $\pm$ 0.03
FCC 043	03 26 02.2	-32 53 40	13.91	0.06	+1337	-0.02	-17.5	16.9	56	-0.25 $\pm$ 0.03
FCC 046	03 26 25.0	-37 07 41	15.99	0.08	+2252	-0.03	-16.6	6.7	61	+0.18 $\pm$ 0.05
FCC 136	03 34 29.5	-35 32 47	14.81	0.07	+1238	-0.02	-16.5	14.2	64	-0.48 $\pm$ 0.04
FCC 150	03 35 24.1	-36 21 50	15.70	0.06	+2000	-0.03	-16.6	5.7	63	-0.56 $\pm$ 0.04
FCC 204	03 38 13.6	-33 07 38	14.76	0.04	+1368	-0.02	-16.7	11.5	67	-0.40 $\pm$ 0.03
FCC 207	03 38 19.3	-35 07 45	16.19	0.06	+1429	-0.02	-15.4	8.4	60	-0.31 $\pm$ 0.04
FCC 245	03 40 33.9	-35 01 23	16.00	0.05	+2180	-0.03	-16.5	11.4	39	-0.45 $\pm$ 0.04
FCC 266	03 41 41.4	-35 10 12	15.90	0.05	+1546	-0.02	-15.9	7.1	42	-0.61 $\pm$ 0.03
FCC 288	03 43 22.6	-33 56 25	15.10	0.03	+1087	-0.02	-15.9	9.5	48	+0.12 $\pm$ 0.03
FS 029	13 13 56.2	-16 16 24	15.70	0.28	+2447	-0.04	-17.3	8.9	59	-0.24 $\pm$ 0.02
FS 075	13 15 04.1	-16 23 40	16.87	0.31	+1889	-0.03	-15.6	6.8	49	-0.45 $\pm$ 0.02
FS 076	13 15 05.9	-16 20 51	16.10	0.30	+2698	-0.04	-17.1	4.4	56	-0.34 $\pm$ 0.02
FS 131	13 16 49.0	-16 19 42	15.30	0.35	+2556	-0.04	-17.8	8.1	87	-0.13 $\pm$ 0.02
FS 373	10 37 22.9	-35 21 37	15.60	0.49	+2444	-0.04	-17.6	7.9	73	-0.46 $\pm$ 0.04
NGC 5898_DW1	15 18 13.0	-24 11 47	15.66	0.61	+2467	-0.04	-17.7	8.7	43	+0.02 $\pm$ 0.02
NGC 5898_DW2	15 18 44.7	-24 10 51	16.10	0.66	+1993	-0.03	-16.8	5.9	44	-0.05 $\pm$ 0.03

[a] from HyperLeda database (Prugniel & Simien, 1996);[b] from Simien & Prugniel (2002);[c] from Koleva (2009); [d] from Vazdekis et al. (2001)

2.4 Analysis

The SSP-equivalent profiles (see Fig. 1, 2 of Koleva et al. 2009a) were obtained by binning the 2D spectrum in the spatial direction to achieve a signal-to-noise ratio of 20 and by analysing the resulting 1D spectra with ULySS[2] (Université de Lyon Spectroscopic analysis Software, Koleva et al., 2009b).

ULySS is designed to fit any linear combination of non-linear components (weighted by W) against a spectrum $F_{obs}(\lambda)$. A model constructed as such, can be convolved with a line-of-sight velocity distribution (LOSVD) and multiplied by a n^{th} order Legendre polynomial, $P_n(\lambda)$.:

$$F_{obs}(\lambda) = P_n(\lambda) \times \Big(\mathrm{LOSVD}(v_{sys}, \sigma, h3, h4) \otimes \sum_{i=0}^{i=k} W_i \ \mathrm{CMP}_i\,(a_1, a_2, ..., \lambda) \Big). \quad (1)$$

The LOSVD is a function of the systemic velocity, v_{sys} and the velocity dispersion σ and may include a Gauss-Hermit expansion ($h3$ and $h4$, van der Marel & Franx, 1993). λ is the logarithm of the wavelength (the logarithmic scale is required to express the effect of the LOSVD as a convolution). In this particular case, the CMP ($i = 1$) is a SSP constructed with Pégase.HR stellar population models (Le Borgne et al., 2004) using Elodie.3.1 empirical stellar library (Prugniel & Soubiran, 2001; Prugniel et al., 2007b). Consequently, the parameters a_1, a_2 are the age and metallicity of the SSP. For the α-elements analysis we added another parameter a_3 which expresses the $[Mg/Fe]$ abundance. In the latter case the stellar population models were build with a semi-empirical library, produced by combination of Elodie.3.1 and Coelho et al. (2005) libraries, including the non-solar abundance of $[Mg/Fe]$ (Prugniel et al., 2007a; Koleva et al., 2008). More precisely, Elodie.3.1 was differentally corrected for $[Mg/Fe]$ = 0.0 and 0.4, using Coelho et al. library. The analysis selects the optimal $[Mg/Fe]$ value interpolated in this range.

Some of the galaxies formation models predict relation between the mass of a galaxy and its metallicity gradient. As a proxy to the mass we used the velocity dispersion and the absolute magnitude. We took the velocity dispersion values from the literature (see Table1). The absolute magnitudes were computed using cz, m_B (from Table1) and Hubble constant $H_0 = 70$ km s^{-1} Mpc^{-1}. We corrected for Schlegel et al. (1998) galactic extinction and reddening (de-

[2] http://ulyss.univ-lyon1.fr

© 2009 WILEY-VCH Verlag GmbH & Co. KGaA, Weinheim

rived with ABG and COCOR respectively from the PLEINPOT[3] package).

We did not find any obvious correlation between our gradients and the mass of the galaxies. From Fig. 1 one can notice that if we had data only from Vazdekis et al. (2001) and several dwarfs from Koleva et al. (FCC 288, DW 1, DW 2, FS 131) then we could have found a mass-gradient relation. We note also that, some of our flattest galaxies ($\epsilon > 0.3$; DW 1, DW 2, FCC 046, FCC 288, FS 029, FS 131) follow a trend with M_B and σ. However, FCC 204, which is also flat ($\epsilon = 0.61$), is an outlier. We cannot exclude the possibility that the contrasting results are due to the small size of the sample or to the actual selection critreria.

3 Validation

3.1 Noise and sky subtraction

The two main features of the data reduction and analysis which can affect the derived metallicity gradients are a possible bad sky subtraction and the decreasing signal-to-noise from the centre to the outskirts. Our measurements are almost insensitive to flux calibration problems (as the Lick indices). The shape of the flux is modeled by a multiplicative polynomial, during the fitting and cannot be a source of biases.

To investigate how the signal-to-noise and imperfections of the sky subtraction can affect the measured metallicities, we produced a 1D model of the centre of FS 373, using the Pégase.HR population synthesis code. The choice of this particular galaxy, was driven by the its strong metallicity gradient (-0.46 dex). To construct the model, we use the SSP-equivalent parameters as derived from our analysis, *i.e.* age = 1.55 Gyr and $[Fe/H]$ = 0.0 dex. We broadened the model to the velocity dispersion (instrumental plus physical) of the observed spectrum.

To investigate the metallicity dependence on the S/N we added Gaussian noise to the model using SNR and NSIMUL keywords in the call of ULySS. The results are shown in Fig. 2. The errors become larger when the S/N decreases, an expected behaviour. However, we do not observe any important systematics in the measured metallicity values down to S/N = 10.

The sky subtraction, especially for diffuse objects like the dwarf galaxies, is a particularly critical point. To obtain a negative metallicity gradient, one needs to systematically under-subtract the background. To explore this effect, we took an UVES sky spectrum (Hanuschik , 2003) and broadened it to the instrumental resolution of FORS2, 74 km s^{-1}, and scaled it to the typical brightness of the dark sky. Taking into account the redshift of the galaxy we added the two spectra (sky plus galaxy). We simulated an under-subtraction of the sky from fully subtracted to unsubtracted. The results are shown in Fig. 3. To decrease the gradients by 0.2 dex, we need to under-subtract 50 % of the sky. For FS 373, where the gradient is -0.46 dex, we would need to under-estimate the sky by more than 100 %! We could possibly make an error on the sky subtraction of 10 % in improbable cases, but certainly not as a systematic under-subtraction. Our strong gradients cannot be an artifact of a bad sky subtraction. At least not in the way we modeled it here.

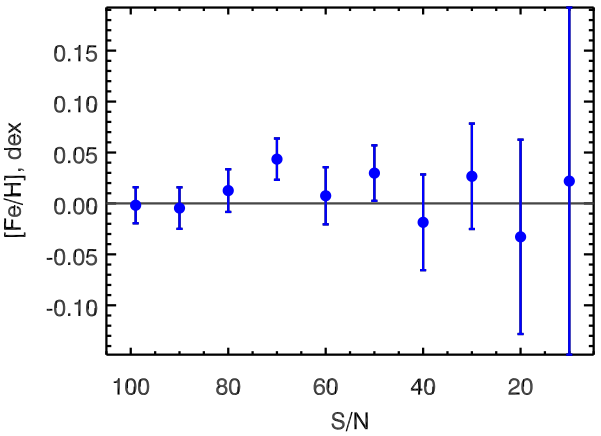

Fig. 2 Dependence of the ULySS metallicity determination on the signal-to-noise of the data. With grey line we plot the input metallicity and with blue filled circles the output values of $[Fe/H]$.

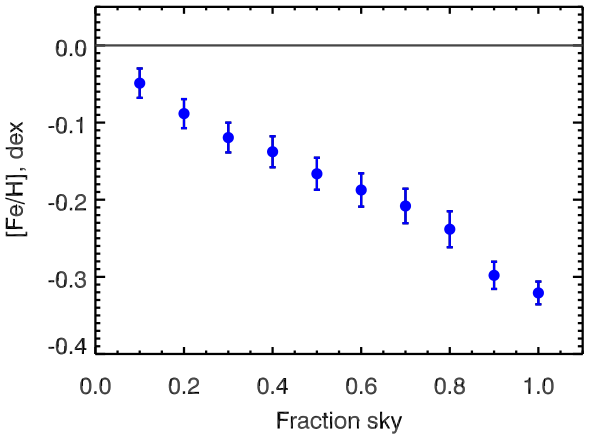

Fig. 3 Dependence of the metallicity determination with ULySS on the under-subtracted sky in fraction. The grey line marks the input metallicity of the model, while the blue dots are the derived metallicity. In abscisse, fraction = 1 corresponds to the non subtraction of the sky, and fraction = 0 to the exact subtraction.

[3] http://leda.univ-lyon1.fr/pleinpot/pleinpot.html

© 2009 WILEY-VCH Verlag GmbH & Co. KGaA, Weinheim

3.2 Iron against metallicity abundance

The metallicity of the stellar population models are labeled in $[Fe/H]$ (because the stellar libraries are indexed in this manner). Therefore, although the stellar evolution depends on the detailed abundance (Salasnich et al., 2000), the full-spectrum fitting measures $[Fe/H]$ rather than $[Z/H]$ (the differences in the stellar evolution mostly translates as biases on the age).

Spolaor et al. using Thomas et al. 2004 models, derived their $[Z/H]$ as a sum of Fe-like plus Mg-like elements (*C, N, O, Mg, Na, Si*). Consequently, if the populations are not scaled-solar, the results may not be consistent with ours.

To make the comparison rigorous, we also derived $[Z/H]$ by measuring $[Mg/Fe]$. We explore the possibility that the $[Mg/Fe]$ gradients compensate $[Fe/H]$ to result in flat $[Z/H]$ profiles. To test the difference in the measured quantities we used our α-enhanced models (Prugniel et al., 2007a; Koleva et al., 2008) as explained in Sect. 2. We found in general negative $[Mg/Fe]$ gradients ($\Delta[Mg/Fe] = -0.10 \pm 0.09$ dex). Only four galaxies (DW 1, FS 76, FS 131, FCC 043) have flat or positive $[Mg/Fe]$ gradient. We computed the total metallicity using $[Z/H] = [Fe/H] + 0.98\ [Mg/Fe]$ (Thomas et al., 2004). We find that the total metallicity gradients (see Fig.4) are *stronger* than the $[Fe/H]$ gradients, and the difference in the metallicity definitions cannot explain the difference between the two data sets.

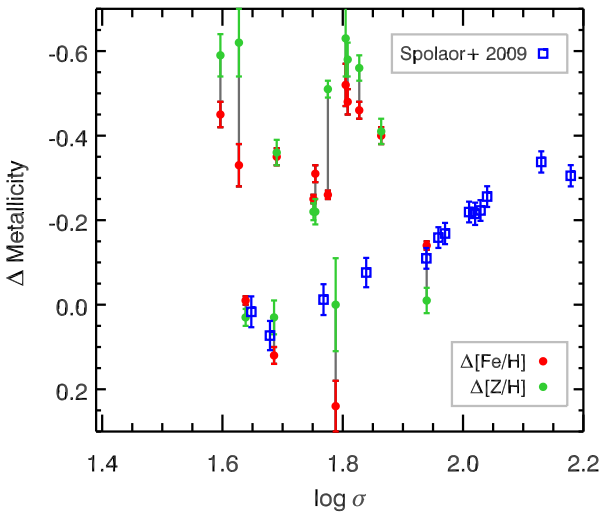

Fig. 4 Relation between $[Fe/H]$ (red filled circles) and $[Z/H]$ (green filled circles) gradients for the FORS dwarf ellipticals. The gradients of each galaxies are connected with a line. The sample of Spolaor et al. is plotted with blue open squares.

4 Discussions

We investigated the discrepancy in the metallicity gradients-mass relation between two recent works, namely Spolaor et al. (2009) and Koleva et al. (2009a). While the former work shows a very strong and tight relation between the total metallicity gradient in low-mass galaxies and their central velocity dispersion or M_B, the latter do not find a hint of such a relation.

As first guess for this discrepancy we pointed the small size of the samples and different selection criteria. Such a scenario is possible, since some of our galaxies fall on Spolaor et al. relation. This hypothesis may be supported by the fact that the Fornax galaxies of Spolaor et al. (2009) are in general flat ($\epsilon > 0.3$), and we have shown that the gradients in such galaxies are usually shallower. However, in their Virgo sample all but one galaxy have $\epsilon < 0.3$[4]. Hence, this explanation is ruled out and flattening cannot be a reason for our disagreement.

Another possible explanation would have been that while the dwarf galaxies exhibit a strong negative $\Delta[Fe/H]$, they possess the same $[\alpha/Fe]$ gradient but with a positive sign. Thus, measuring the total metallicity as a combination of $[Fe/H]$ and $[\alpha/Fe]$, we would have a total $\Delta[Z/H] = 0$. We measured the $[Mg/Fe]$ gradients in our sample using unpublished semi-empirical models (Prugniel et al., 2007a). These models are preliminary but the relative measurements of $[Mg/Fe]$ are certainly reliable. Opposite to the expectations we found that (most of) our galaxies possess *negative* $[Mg/Fe]$ gradients. Consequently, the total metallicity gradients are *stronger* than the $[Fe/H]$ gradients.

Negative iron and $[Mg/Fe]$ gradients will imply that, in the early epochs, when the feedback is a strong regulator, the star formation starts in the centre, where the gas is the densest. After the gas is exhausted, the star formation stops first in the centre and continues longer at larger radius. This process forming a negative $[Mg/Fe]$ gradient. To form the negative $[Fe/H]$ gradient we need that cool, enriched gas flows again into the centre, triggering star formation. In other words, having repeating episodes of star formation. This scenario is in agreement with recent SPH simulations on the formation of dwarf galaxies (Valcke et al., 2008, fig.10)

We also investigated the effect of a bad sky-subtraction and low signal-to-noise on our metallicity measurements. We showed that our metallicity measurements are not biased down to S/N = 10 and that to have zero metallicity gradients we need to under-subtract the sky with more than 50 %. We concluded that these two effects cannot be the cause of our strong gradients.

As a conclusion, according to the tests performed in this paper, the origin of the differences between the two articles remains unknown.

[4] We used the ellipticity measurements from the HyperLeda database (Paturel et al., 2003), http://leda.univ-lyon1.fr

© 2009 WILEY-VCH Verlag GmbH & Co. KGaA, Weinheim

Acknowledgements. We thank the organizers for the fruitful meeting. We thank Patricia Sánchez-Blázquez for the useful discussions. MK has been supported by the Programa Nacional de Astronomía y Astrofísica of the Spanish Ministry of Science and Innovation under grant *AYA2007-67752-C03-01* and Bulgarian Scientific Research Fund *DO 02-85/2008*. We used DEXTER (http://dc.zah.uni-heidelberg.de/sdexter) to acquire the measurements from published figures.

References

Arimoto N., Yoshii Y., 1987, A&A, 173, 23
Coelho P., Barbuy B., Meléndez J., Schiavon R. P., Castilho B. V., 2005, A&A, 443, 735
Cole S., Aragon-Salamanca A., Frenk C. S., Navarro J. F., Zepf S. E., 1994, MNRAS, 271, 781
De Rijcke S., Michielsen D., Dejonghe H., Zeilinger W. W., Hau G. K. T., 2005, A&A, 438, 491
di Matteo P., Pipino A., Lehnert M. D., Combes F., Semelin B., 2009, A&A, 499, 427
Hanuschik R. W., 2003, A&A, 407, 1157
Kawata D., Gibson B. K., 2003, MNRAS, 340, 908
Koleva, M., 2009, PhD thesis
Koleva M., Gupta R., Prugniel P., Singh H., 2008, in Astronomical Society of the Pacific Conference Series, Vol. 390, Pathways Through an Eclectic Universe, Knapen J. H., Mahoney T. J., Vazdekis A., eds., pp. 302
Koleva M., de Rijcke S., Prugniel P., Zeilinger W. W., Michielsen D., 2009a, MNRAS, 396, 2133
Koleva M., Prugniel P., Bouchard A., Wu Y., 2009b, A&A, 501, 1269
Larson R. B., 1974, MNRAS, 166, 585
Le Borgne D., Rocca-Volmerange B., Prugniel P., Lançon A., Fioc M., Soubiran C., 2004, A&A, 425, 881
Matteucci F., Tornambe A., 1987, A&A, 185, 51
Paturel G., Petit C., Prugniel P., Theureau G., Rousseau J., Brouty M., Dubois P., Cambrésy L., 2003, A&A, 412, 45
Proctor R. N., Sansom A. E., 2002, MNRAS, 333, 517
Prugniel P., Koleva M., Ocvirk P., Le Borgne D., Soubiran C., 2007a, in IAU Symposium, Vol. 241, IAU Symposium, Vazdekis A., Peletier R. F., eds., pp. 68–72
Prugniel Ph., Simien F., 1996, A&A, 309, 749
Prugniel P., Soubiran C., 2001, A&A, 369, 1048
Prugniel P., Soubiran C., Koleva M., Le Borgne D., 2007b, arXiv:astro-ph/0703658
Salasnich B., Girardi L., Weiss A., Chiosi C., 2000, A&A, 361, 1023
Sánchez-Blázquez P., Gorgas J., Cardiel N., 2006, A&A, 457, 823
Schlegel D. J., Finkbeiner D. P., Davis M., 1998, ApJ, 500, 525
Simien F., Prugniel P., 2002, A&A, 384, 371
Spolaor M., Proctor R. N., Forbes D. A., Couch W. J., 2009, ApJ, 691, L138
Thomas D., Maraston C., Korn A., 2004, MNRAS, 351, L19
Valcke S., de Rijcke S., Dejonghe H., 2008, MNRAS, 389, 1111
van der Marel R. P., Franx M., 1993, ApJ, 407, 525
Vazdekis A., Kuntschner H., Davies R. L., Arimoto N., Nakamura O., Peletier R., 2001, ApJ, 551, L127
White S. D. M., 1980, MNRAS, 191, 1P
Worthey G., Faber S. M., Gonzalez J. J., Burstein D., 1994, ApJS, 94, 687
Worthey G., Ottaviani D. L., 1997, ApJS, 111, 377

© 2009 WILEY-VCH Verlag GmbH & Co. KGaA, Weinheim